Rev. Roum. Sci. Techn.– Électrotechn. et Énerg.
Vol. **66**, *5*, pp. 225–230, Bucarest, 2021

AN EFFICIENT HYBRID CONVERTER FOR DC-BASED RENEWABLE ENERGY NANOGRID SYSTEMS

ANNAPOORANI SUBRAMANIAN[1], JAYAPARVATHY RAMAN[2], NAMMALVAR PACHAIVANNAN[3]

Key words: Boost converter, Dc nanogrid, Hybrid converter, Photovoltaic panel, Single input multiple output converter.

Many electrical and electronic equipment used in homes requires multiple dc and ac power supplies. Existing hybrid converters used in nanogrid systems provide only single ac and dc outputs for single dc input. They also have limitations such as shoot through problem and requirement of dead time circuitry. This paper proposes a novel single input multiple output hybrid converter (SIMOHC) derived from the dc-dc boost converter, which can produce one ac and two dc outputs simultaneously in single stage from a single dc input with less complex circuit. The proposed converter has higher electromagnetic interference (EMI) immunity, no shoot through problem, and dead time circuitry requirement is avoided. The proposed converter uses simple unipolar sinusoidal pulse width modulation (USPWM) technique and provides higher reliability. The proposed converter is validated using simulation and hardware implementation. It is observed that the proposed circuit performs equally good compared to the existing hybrid converter like boost derived hybrid converter (BDHC), and in addition, has the advantage of providing two dc outputs and one ac output.

1. INTRODUCTION

The uncertainty and cost involved with fossil fuels necessitate the use of renewable energy resources in numerous applications [1]. Modern electronic appliances like mobile chargers, laptop chargers, and LED driver circuits need power electronic circuit interface. Decentralized distribution has increased demand in residential and industrial buildings due to its smooth control flexibility. This structure in literature [2,3] is termed as nanogrid. Nanogrid type architecture is also used to feed different loads in hybrid electric vehicles (HEV) [4,5]. The nanogrid architecture is of two types depending upon the source as dc nanogrid and ac nanogrid [6]. This paper focuses on dc nanogrid, which is fed from dc source only. In conventional dc nanogrid architecture, two dedicated converters are used for the dc-dc and dc-ac conversion, which involves more switches and associated losses. For dc-dc conversion, boost converter may be used, and for dc-ac conversion, mostly, voltage source inverter (VSI) is used, which has less reliability due to EMI or other noise signals resulting in the shoot-through condition, that occurs when switches in the same leg are turned on simultaneously. Hybrid converter is a single stage converter, which can feed ac and dc loads simultaneously with a smaller number of switches.

The advantages of hybrid converters are high reliability due to inherent shoot-through protection, compact size, high EMI immunity, and no need of dead time circuitry, which increases its suitability for loads which need both dc and ac supply. An ac fan and a LED lamp in a home can be fed simultaneously from a hybrid converter in a single stage. Renewable energy sources provide clean and green energy, and hence, preferred for intelligent residential applications. Among all renewable energy sources, PV panels or fuel cells are preferred as sources for dc-based systems. Low voltage and power ratings are the drawbacks of renewable energy sources. Topologies with high boosting factor are required to produce step up operation based on the requirements [7,8]. Therefore, various configurations of single stage boost converters are proposed for hybrid converters, which can feed ac and dc loads at the same time.

Shoot-through is the major problem in the conventional VSIs, which requires the use of dead time circuitry. Unwanted turning on of the inverter leg switches due to the spurious noise signals or EMI causes damage to the switches. Hence, VSI when used in residential applications must be provided with proper protection against EMI or other spurious signals. In Z-source inverter (ZSI), the problem of shoot-through is mitigated [9]. Due to the presence of input impedance network in ZSI, both the switches of the inverter leg can be turned on at the same time, which is called the shoot-through state. To increase the boosting factor, extended boost ZSI [10] is presented in Z-source topology. But the drawback with ZSI is that it cannot supply both ac and dc loads at the same time. Also, dynamic instability is caused when two capacitors are not matched across them with equal loads [11]. Based on inverse Watkins–Johnson (IWJ) topology, a hybrid converter called Switched Boost Inverter (SBI) is presented in [12]. Other than the components in VSI, SBI has two switches and one pair of LC filter, but could supply both dc and ac load simultaneously, and has the advantages of ZSI like buck-boost operation and allowing shoot-through of the inverter switches to provide EMI immunity.

Boost derived hybrid converter (BDHC) [13,14] is proposed from the boost converter, which is based on the two switch converter. Component count is less in BDHC in comparison to IWJ converter. A hybrid converter based on current fed switched inverter (CFSI) based hybrid converter presented in [15] feeds both ac and dc loads simultaneously from a single dc supply, and has high boosting voltage making it suitable for dc nanogrid systems. Residential loads may need two dc outputs and one ac output like two LEDs and one ac fan. Hence, this paper proposes a single input multiple output hybrid converter (SIMOHC) based on the boost converter, which can produce two dc outputs and one ac output simultaneously with a smaller number of switches in single stage. The simple and conventional

[1]Agni College of Technology, Thalambur, Tamil Nadu, India, tannapoorani@gmail.com
[2]Sri Sivasubramaniya Nadar College of Engineering, Kalavakkam, Tamil Nadu, India
[3]Krishnasamy College of Engineering and Technology, Cuddalore, India

USPWM technique could be used to produce the required ac and dc voltages.

The main contribution of this paper includes,

1. Two dc outputs and one ac output in a hybrid converter.
2. Reduced switch/diode count.
3. Increased reliability since there is no shoot-through problem.
4. No need of dead time circuitry.
5. Simple USPWM technique can be employed.

The outline of this paper is as follows. In Section 2, the proposed circuit, and its modes of operation with the steady state analysis are presented. Section 3 explains the closed loop operation to regulate both ac and dc outputs. Section 4 provides the simulation results. Section 5 presents the experimental results, and the conclusions are presented in the last section.

2. PROPOSED SIMOHC TOPOLOTY

2.1. OPERATION OF PROPOSED CIRCUIT AND ITS MODES

The conventional boost converter is presented in Fig. 1.

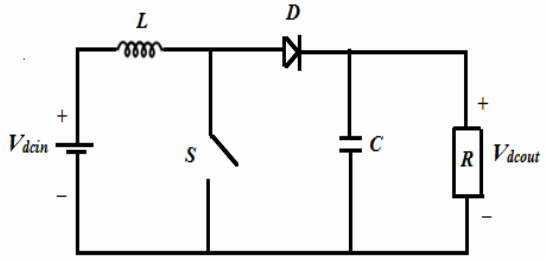

Fig. 1 – Conventional boost converter.

The proposed SIMOHC consists of two input capacitors C_1 and C_3, two output capacitors C_2 and C_4, two inductors for boosting L_1 and L_2, four IGBT switches S_1, S_2, S_3, and S_4, two diodes D_1 and D_2, freewheeling diodes, FD_1, FD_2, FD_3, and FD_4 across the IGBT switches, and produces one ac output voltage, V_{acout} and two dc output voltages V_{dcout1} and V_{dcout2} with the dc input voltage V_{dcin}.

SIMOHC is obtained by connecting the two boost converters to the same input and adding an IGBT switch in series before the inductor in each boost converter as shown in Fig. 2. The ac load is connected between the junction of L_1, S_4, and D_1 and the junction of L_2, S_3, and D_2, and the ac output voltage is represented as V_{acout}. The boosted dc outputs V_{dcout1} and V_{dcout2} are taken across the capacitors C_2 and C_4 respectively.

The continuous conduction mode has been assumed in this paper, where the load current will not become zero in between. The operation of the proposed converter is explained in two modes, namely mode I and mode II.

Mode I. During this mode, switches S_1 and S_3 are in the on condition, and switches S_2 and S_4 are in the off condition. The current starts flowing from the positive terminal of input voltage, then flows through S_1, L_1, and then, the current branches into two paths – one path of current is via D_1 and produces one dc output voltage, V_{dcout1}, and returns to the negative terminal of the input voltage and the second path of current is via ac load producing V_{acout}, and then the current passes through S_3 and returns to the negative terminal of the input voltage. The charged capacitor C_4 will feed the second dc load, V_{dcout2}. The equivalent circuit during Mode I operation is shown in Fig. 3a.

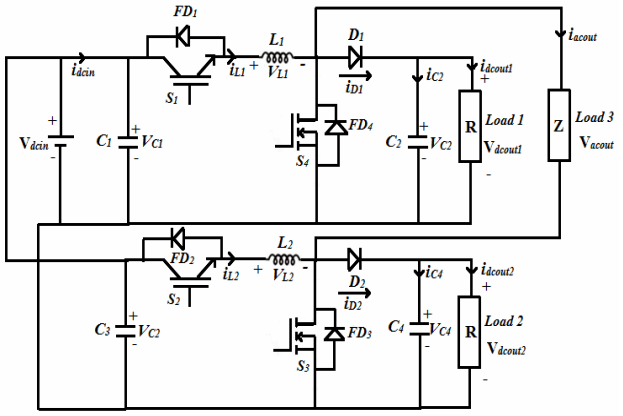

Fig. 2 – Proposed SIMOHC obtained by connecting two boost converters to the same input and adding a switch in series before inductor in each boost converter.

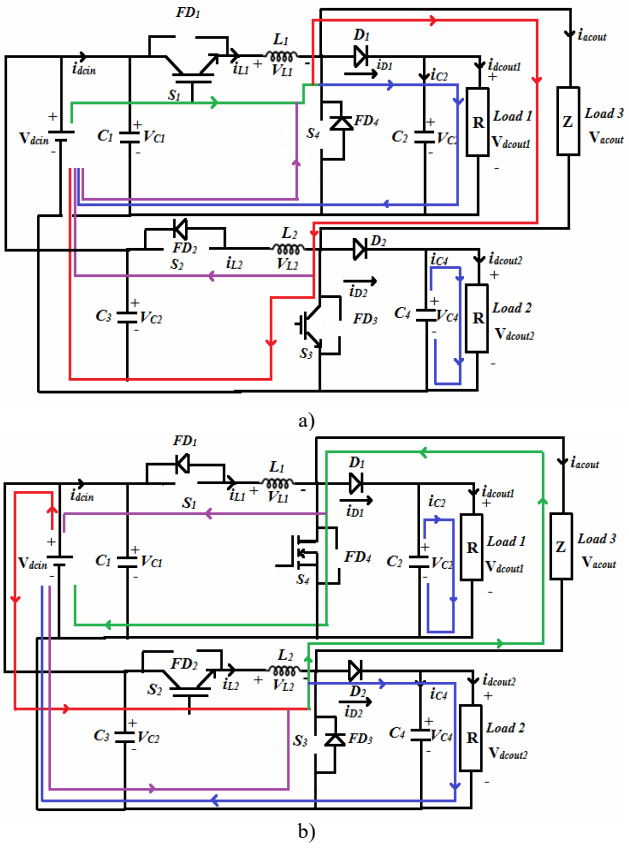

a)

b)

Fig. 3 – a) Equivalent circuit of SIMOHC during mode I operation; b) equivalent circuit of SIMOHC during mode II operation.

Mode II. During this mode, switches S_2 and S_4 are in the on condition, and switches S_1, S_3 are in the off condition. The current starts flowing from the positive terminal of input voltage, then flows through S_2, L_2, and then, the current branches into two paths – one path of current is via D_2 and produces V_{dcout2} and returns to the negative terminal of the input voltage, and second path of current is via ac load producing V_{acout}, and the current flows through S_4 and returns to the negative terminal of the input voltage. The charged capacitor C_2 will feed the first dc load, V_{dcout1}. The equivalent circuit during Mode II operation is shown in Fig. 3b.

2.2. STEADY STATE ANALYSIS

The dc output voltages can be controlled and regulated by controlling the duty cycle, D, as in the case of a boost converter, since SIMOHC combines two boost converters.

The currents through inductors L_1 and L_2 and voltage across capacitors C_2 and C_4 are assumed to have low ripple, and the voltage gain equation for dc output voltages are like that of the boost converter and can be written as,

$$\frac{V_{dcout1}}{V_{dcin}} = \frac{1}{1-D}, \tag{1}$$

$$\frac{V_{dcout2}}{V_{dcin}} = \frac{1}{1-D}, \tag{2}$$

where, $D = T_{on}/T$, T_{on} = on period of switches S_1 and S_3 or S_2 and S_4. The total time-period T determines the frequency of the output ac voltage signal. The ac output voltage can be controlled and regulated by controlling the amplitude modulation index, M as in the case of VSI. Amplitude modulation index is the ratio of amplitude of control signal to the amplitude of high frequency carrier signal. Therefore, the voltage gain expression for ac output voltage [14] can be written as

$$\frac{V_{acout}}{V_{dcin}} = \frac{M}{1-D}. \tag{3}$$

The voltage gain in the dc side in SIMOHC is in the range two to five like a boost converter. The ac gain increases with the modulation index. To get higher voltage gain in the ac side, a step-up transformer may be connected at the ac side before the load. The power output expressions for dc and ac side are denoted as P_{dc} and P_{ac} respectively and can be obtained from equations (1) and (3) as,

$$P_{dc} = \frac{v_{dcin}^2}{R_{dc} \times (1-D)^2}, \tag{4}$$

$$P_{ac} = \frac{0.5 \times v_{dcin}^2 \times M^2}{R_{ac} \times (1-D)^2}, \tag{5}$$

where, R_{ac} and R_{dc} are the resistances in the ac and dc side of output respectively. From the power output equations, the ac output power depends on both the duty cycle and modulation index, whereas the dc output power depends only on the duty cycle. Here, duty cycle is determined by the ON period of switches S_1 and S_3 or S_2 and S_4 during the positive and negative half cycles of ac output voltage V_{acout}. The steady state analysis of the SIMOHC can be obtained by considering the equivalent circuit as shown in Fig. 4a and Fig. 4b as follows,

During the interval (0 – T/2),

$$V_{dcin} = L_1 \frac{\mathrm{d}i_{L1}}{\mathrm{d}t} + i_{dcout1} R_1, \tag{6}$$

$$R_1 i_{dcout1} - R_3 i_{acout} = 0. \tag{7}$$

From equation (6)

$$\frac{V_{dcin}}{L_1} - \frac{i_{dcout} R_1}{L_1} = \frac{\mathrm{d}i_{L1}}{\mathrm{d}t}, \tag{8}$$

$$i_{L1} = i_{dcout1} + i_{acout}, \tag{9}$$

$$i_{dcout1} = i_{L1} - i_{acout}. \tag{10}$$

Substituting eq. (10) in eq. (8),

$$\frac{\mathrm{d}i_{L1}}{\mathrm{d}t} = \frac{V_{dcin}}{L_1} - \frac{i_{L1} R_1}{L_1} + \frac{i_{acout} R_1}{L_1}. \tag{11}$$

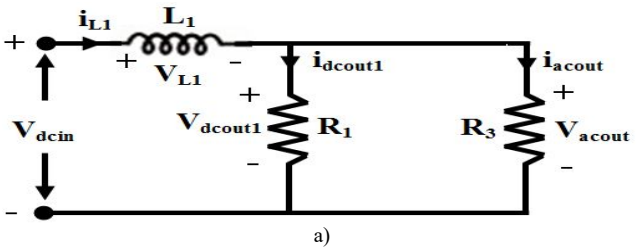

a)

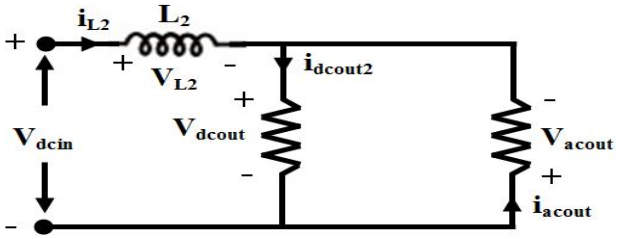

b)

Fig. 4 – a) Equivalent circuit during (0 – T/2) interval; b) equivalent circuit during (T/2– T) interval.

State equation during (0 – T/2) interval is

$$\begin{bmatrix} \dot{i}_{L1} \\ \dot{i}_{L2} \end{bmatrix} = \begin{bmatrix} \frac{-R_1}{L_1} & 0 \\ 0 & 0 \end{bmatrix} \begin{bmatrix} i_{L1} \\ i_{L2} \end{bmatrix} + \begin{bmatrix} \frac{R_1}{L_1} \\ 0 \end{bmatrix} \begin{bmatrix} i_{acout} \\ 0 \end{bmatrix} + \begin{bmatrix} \frac{1}{L_1} \\ 0 \end{bmatrix} [V_{dcin}], \tag{12}$$

The output equation during (0 – T/2) interval is

$$\begin{bmatrix} V_{dcout\,1} \\ V_{dcout\,2} \\ V_{acout} \end{bmatrix} = \begin{bmatrix} R_1 & 0 & 0 \\ 0 & 0 & 0 \\ 0 & 0 & R_3 \end{bmatrix} \begin{bmatrix} i_{dcout\,1} \\ i_{dcout\,2} \\ i_{acout} \end{bmatrix} \tag{13}$$

From equations (12) and (13),

$$A_1 = \begin{bmatrix} \frac{-R_1}{L_1} & 0 \\ 0 & 0 \end{bmatrix}; \; B_1 = \begin{bmatrix} \frac{1}{L_1} \\ 0 \end{bmatrix}; \; C_1 = \begin{bmatrix} R_1 & 0 & 0 \\ 0 & 0 & 0 \\ 0 & 0 & R_3 \end{bmatrix} \tag{14}$$

During the interval (T/2 – T),

$$V_{dcin} = i_{L2} \frac{\mathrm{d}i_{L2}}{\mathrm{d}t} + i_{dcout2} R_2, \tag{15}$$

$$R_2 i_{dcout2} + R_3 i_{acout} = 0, \tag{16}$$

$$i_{L2} = i_{dcout2} - i_{acout}, \tag{17}$$

$$i_{dcout\,2} = i_{L2} + i_{acout}. \tag{18}$$

From eq. (15), we get,

$$\frac{\mathrm{d}i_{L2}}{\mathrm{d}t} = \frac{V_{dcin}}{L_2} - i_{L2} \frac{R_2}{L_2} - \frac{i_{acout} R_2}{L_2}. \tag{19}$$

The state equation during the interval (T/2 – T) is

$$\begin{bmatrix} \dot{i}_{L1} \\ \dot{i}_{L2} \end{bmatrix} = \begin{bmatrix} 0 & 0 \\ 0 & \frac{-R_2}{L_2} \end{bmatrix} \begin{bmatrix} i_{L1} \\ i_{L2} \end{bmatrix} + \begin{bmatrix} 0 \\ \frac{-R_2}{L_2} \end{bmatrix} \begin{bmatrix} 0 \\ i_{acout} \end{bmatrix} + \begin{bmatrix} 0 \\ \frac{1}{L_2} \end{bmatrix} [V_{dcin}] \tag{20}$$

The output equation during this interval is

$$\begin{bmatrix} V_{dcout\,1} \\ V_{dcout\,2} \\ V_{acout} \end{bmatrix} = \begin{bmatrix} 0 & 0 & 0 \\ 0 & R_2 & 0 \\ 0 & 0 & -R_3 \end{bmatrix} \begin{bmatrix} i_{dcout\,1} \\ i_{dcout\,2} \\ i_{acout} \end{bmatrix} \tag{21}$$

From eq. (20) and (21),

$$A_2 = \begin{bmatrix} 0 & 0 \\ 0 & \frac{-R_2}{L_2} \end{bmatrix}; B_2 = \begin{bmatrix} 0 \\ \frac{1}{L_2} \end{bmatrix}; C_2 = \begin{bmatrix} 0 & 0 & 0 \\ 0 & R_2 & 0 \\ 0 & 0 & -R_3 \end{bmatrix} \tag{22}$$

3. CLOSED LOOP OPERATION OF SIMOHC

The simple and conventional USPWM scheme can be utilized for the SIMOHC to get two dc outputs and one ac output simultaneously, which is shown in Fig. 5.

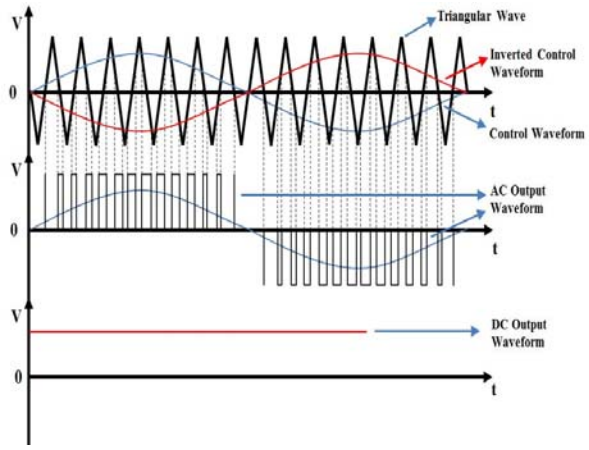

Fig. 5 – Unipolar sinusoidal pulse width modulation scheme.

The closed loop operation of SIMOHC is shown in Fig. 6. For the control of the proposed converter, d-q reference frame [16] is used. The switching signals to S_1, S_2, S_3, and S_4 are obtained from the PWM signal generator using the reference frame theory.

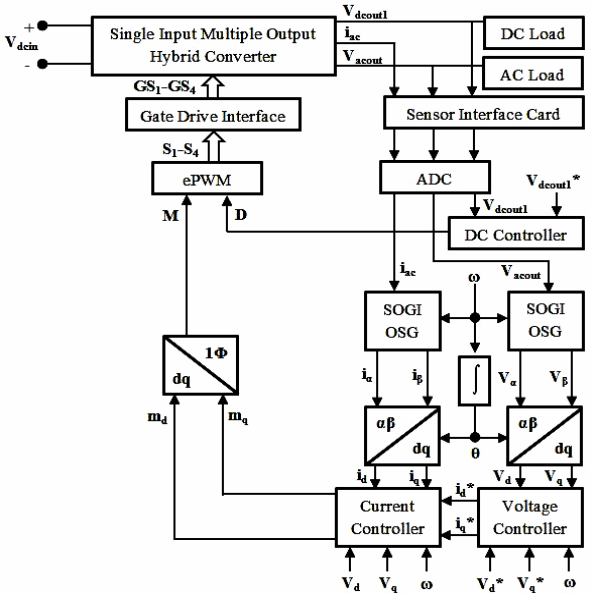

Fig. 6 – Closed loop operation of SIMOHC with d-q control strategy.

The main aim of closed loop control is to obtain the regulation of ac output voltage, V_{acout}, and dc output voltages V_{dcout1} and V_{dcout2} to the reference values. The regulation of V_{dcout1} helps in the regulation of V_{dcout2} since identical load and component values are chosen for the second dc output. The dc output voltage V_{dcout1}, ac output current, i_{ac}, and ac output voltage, V_{acout} are converted to digital signals using analog to digital converter (ADC) through sensor interface card. The dc controller compares the V_{dcout1} with the reference dc output voltage, V_{dcout1}*, and gives the proper duty cycle value, D, as input to the PWM signal generator block. The phase-locked loop (PLL) is implemented using second order generalized integrator (SOGI) for the proposed single phase ac output. SOGI when combined with addition of feedback loop termed as orthogonal signal generator (SOGI-OSG). The i_{ac} and V_{acout} are given as inputs to SOGI-OSG blocks, which generates i_α and i_β, V_α and V_β, which are the ac output currents and voltages in the stationary reference frame. The ac output current and voltage quantities in the stationary reference frame are converted into direct axis and quadrature axis current and voltage values in the synchronously rotating reference frame with angular velocity, ω, namely, i_d and i_q, V_d and V_q respectively. The voltage controller gets V_d, V_q, their reference values, V_d*, V_q* along with the angular velocity, ω as inputs and gives the reference ac current values, i_d*, i_q* as outputs. The current controller receives i_d*, i_q* i_d, i_q, V_d, V_q and ω as inputs and gives the direct axis and quadrature axis modulation index values, namely m_d and m_q as outputs. The dq to single phase transformation block converts the m_d and m_q values to single phase quantity, M, which is the modulation index value corresponding to V_d* and V_q*. According to the D and M values that correspond to regulation of dc and ac output voltages, the switching signals to S_1, S_2, S_3, and S_4 of SIMOHC are set by the PWM signal generator. One control loop for ac voltage regulation and another separate control loop for dc voltage regulation are being used. An outer loop for voltage and inner loop for current is being used for ac side voltage and current control respectively.

4. SIMULATION RESULTS

The SIMOHC, which could be used for dc nanogrid applications, where the input dc voltage is fed from either solar panels or fuel cells, is simulated using MATLAB/SIMULINK software, and the results are presented. The input voltage is set at 100 V dc, which is shown in Fig. 7. The dc output voltages V_{dcout1} and V_{dcout2} are shown in Fig. 8.

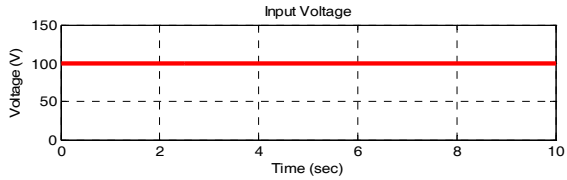

Fig. 7 – Input dc voltage of SIMOHC from the PV panel.

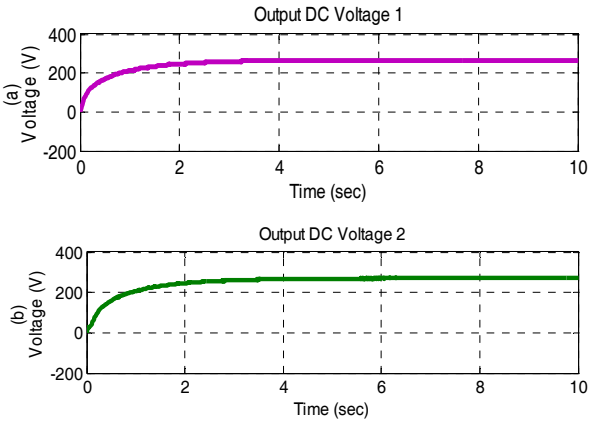

Fig. 8 – Dc output voltages of SIMOHC: a) Dc output voltage 1; b) Dc output voltage 2.

It is observed from simulation that both the dc output voltages are 280 V for a duty cycle of 0.65. The ac output voltage and current are shown in Fig. 9.

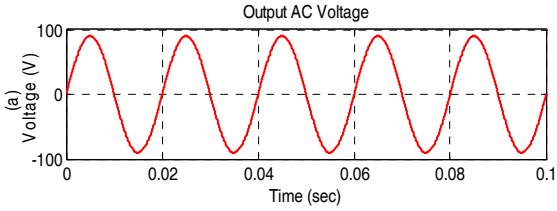

(a)

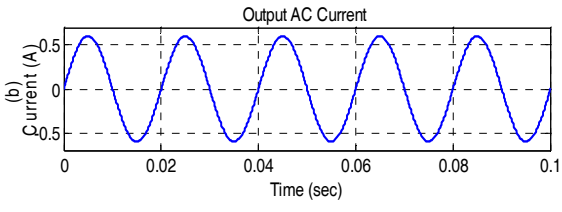

Fig. 9 – Ac outputs: a) AC output voltage; b) Ac output current.

It is observed from simulation that the RMS ac output voltage is 67 V, and the ac output RMS current is 0.4 A with modulation index of 0.35. The performance of the controller under input and output variations for reference dc voltage of 280 V and reference ac voltage of 67 V RMS value is shown in Fig. 10. It is observed from Fig. 10 that the output voltages settle within 0.2 s for the input voltage and load resistance variations.

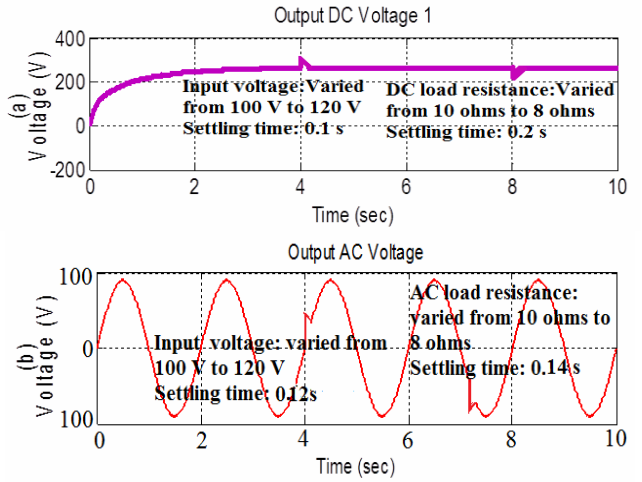

Fig. 10 – Under input and output variations: a) Dc output voltage 1; b) Ac output voltage.

5. EXPERIMENTAL RESULTS

To validate the proposed SIMOHC topology, a hardware prototype is developed and tested. The photograph of the prototype is shown in Fig. 11. The SIMOHC produces one ac output and two dc outputs from a single dc input voltage. Figures 12 a, 12 b, and 12 c and Figs. 13 a, 13 b and 13 c present the output of SIMOHC under steady state condition in open loop. For an input dc voltage of 5 V, the SIMOHC produces dc output voltages of 8 V, 9 V, 12 V for duty cycles of 0.4, 0.5 and 0.6 respectively. The ac output voltage RMS value of 3 V is produced for modulation indexes of 0.6, 0.5, and 0.4 with corresponding duty cycles as 0.4, 0.5, and 0.6 respectively.

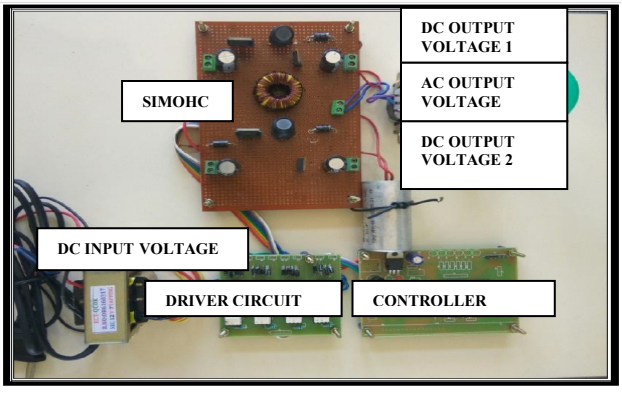

Fig. 11 – Photograph of hardware prototype of SIMOHC.

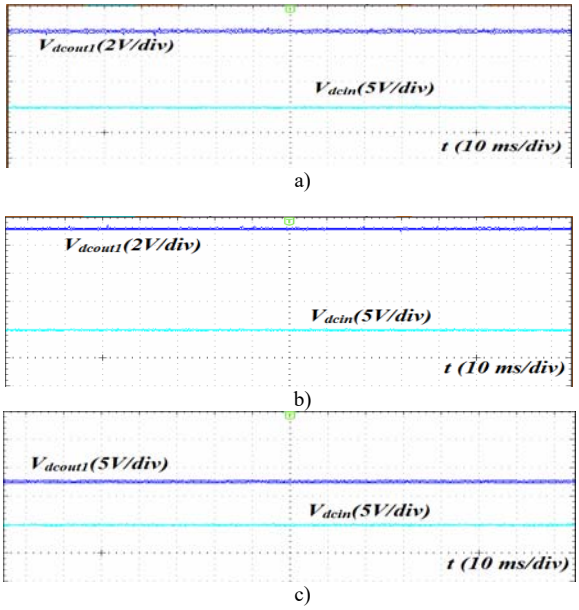

Fig. 12 – Dc input voltage waveform and dc output voltage 1 waveform of SIMOHC: a) duty cycle = 0.4 and modulation index = 0.6; b) duty cycle = 0.5 and modulation index = 0.5; c) duty cycle = 0.6 and modulation index = 0.4.

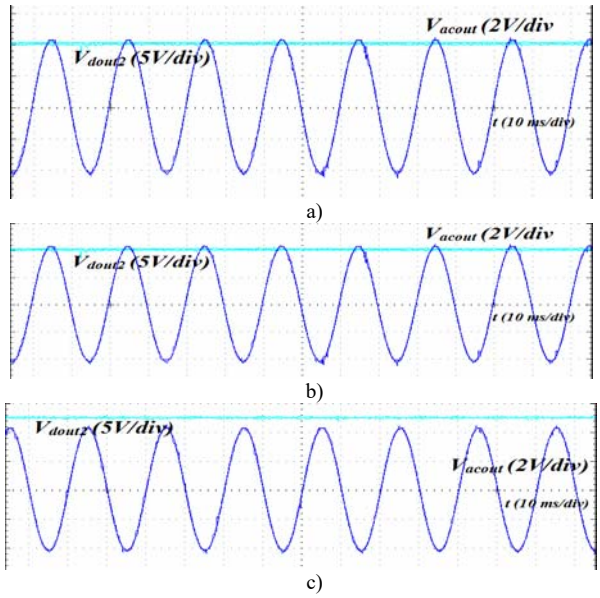

Fig. 13 – Dc output voltage 2 waveform and ac output voltage waveform of SIMOHC: a) duty cycle = 0.4 and modulation index = 0.6; b) duty cycle = 0.5 and modulation index = 0.5; c) duty cycle = 0.6 and modulation index = 0.4.

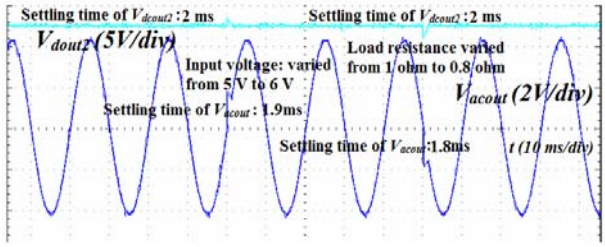

Fig. 14 – Dc output voltage 2 waveform and ac output voltage waveform of SIMOHC under input and output variations.

From Table 1, it is observed that the simulation and experimental results verify the values obtained by the theoretical calculation using eq. (1) and (3). Dc output voltage 2 waveform and ac output voltage waveform of SIMOHC under input and output variations is shown in Fig. 14 for dc reference voltage of 12 V and ac reference voltage of 3 V. It is observed from Fig. 14 that the output

voltages settle within 2 ms for the input voltage and load resistance variations. The controller for the SIMOHC is implemented using DsPIC30F2010 kit. The Table 2 gives the comparison of SIMOHC with other conventional architectures. From Table 2, the dead time circuitry requirement is needed for separate boost and VSI, boost cascaded VSI configurations with five numbers of control elements, and it is not needed for BDHC and SIMOHC configurations with lesser four numbers of control elements.

Table 1

Comparison of simulation and experimental results with theoretical results of SIMOHC

Parameter	Simulation results		Experimental results	
	Theoretical	Actual	Theoretical	Actual
Input voltage (V)	100	100	5	5
Duty Cycle	0.65	0.65	0.6	0.6
Modulation Index	0.35	0.35	0.4	0.4
Output DC voltages (V)	285	280	12.5	12
Output AC voltage (V)	70.7	67	3.535	3
DC voltage gain	2.85	2.8	2.5	2.4

Table 2

Comparison of SIMOHC with other conventional architectures

	Separate Boost and VSI	Boost Cascaded VSI	BDHC	SIMOHC
Total No. of Switches	6	6	5	6
DC Gain	$\frac{1}{1-D}$	$\frac{1}{1-D}$	$\frac{1}{1-D}$	$\frac{1}{1-D}$
Peak AC Voltage	MV_{dcin}	$\frac{M}{1-D}V_{dcin}$	$\frac{M}{1-D}V_{dcin}$	$\frac{M}{1-D}V_{dcin}$
Range of M	$0 \le M \le 1$	$0 \le M \le 1$	$0 \le M \le (1-D)$	$0 \le M \le (1-D)$
Dead Time Requirement	Yes	Yes	No	No
Control Elements	5	5	4	4
No. of Outputs	One AC and one DC Output	One AC and one DC Output	One AC and one DC Output	One AC and two DC Output

All the three configurations in Table 2 except SIMOHC produces only one ac output and one dc output, whereas, SIMOHC produces one ac output and two dc outputs, which makes it more suitable for residential nanogrid applications. The dc output voltage and duty cycle relationship in terms of theoretical and experimental values are shown in Fig. 15. It is noted that the experimental values are nearer to the theoretical values, but little lesser than the theoretical values validating the proposed SIMOHC.

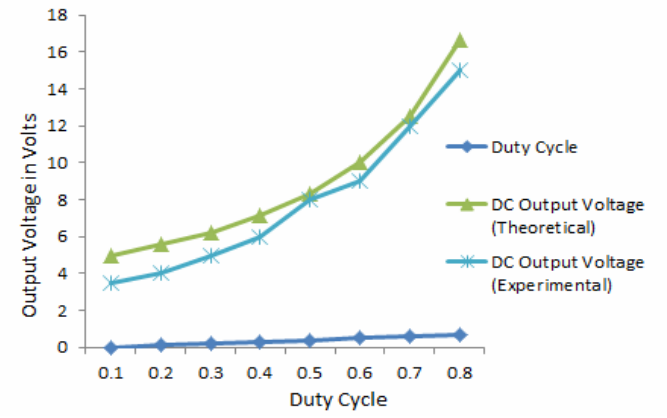

Fig. 15 – Dc output voltage and duty cycle relationship.

6. CONCLUSION

In this paper, a new hybrid converter, SIMOHC, for dc-based nanogrid applications has been proposed, which has the advantages of producing two dc output voltages and one ac output voltage with reduced switch/diode count, increased reliability with no shoot-through problem, and no need of dead time circuitry. The operation of proposed topology and its steady state analysis is presented. The experimental prototype is developed and validated using the simulation results. The conventional and simple USPWM scheme could be employed, which produces ac output voltage that is near sinusoidal. The performance analysis of SIMOHC under transient regime with different controllers can be considered as future work.

Received on May 2, 2020

REFERENCES

1. R. Ramaprabha, S. Malathy, *Dichotomus search-based algorithm for tracking global peak in partial shaded photovoltaic array*, Rev. Roum. Sci. Techn. – Électrotechn. et Énerg., **65**, *3-4*, pp. 211-215, 2020.
2. S.I. Ganesan, D. Pattabiraman, R.K. Govindarajan, M. Rajan, C. Nagamani, *Control scheme for a bidirectional converter in a self-sustaining low-voltage dc nanogrid*, IEEE Trans. Ind. Electron., **62**, *10*, pp. 6317-6326, 2015.
3. J. Schonberger, R. Duke, S.D. Round, *Dc-bus signaling: a distributed control strategy for a hybrid renewable nanogrid*, IEEE Trans. Ind. Electron., **53**, *5*, pp. 1453-1460, 2006.
4. G.-J. Su, L. Tang, A Multiphase, *modular, bidirectional, triple-voltage dc–dc converter for hybrid and fuel cell vehicle power systems*, IEEE Trans. Power Electron., **23**, *6*, pp. 3035-3046, 2008.
5. P. Sun, J.-S. Lai, H. Qian, W. Yu, C. Smith, J. Bates, *High efficiency three-phase soft-switching inverter for electric vehicle drives*, IEEE Vehicle Power and Propulsion Conference, 2000, pp. 761-766.
6. Ó. Lucía, I. Cvetkovic, H. Sarnago, D. Boroyevich, P. Mattavelli, F.C. Lee, *Design of home appliances for a dc-based nanogrid system: an induction range study case*, IEEE J. Emerg. Sel. Top. Power Electron., **1**, *4*, pp. 315-326, 2013.
7. X. Hu, B. Gao, Y. Huang, H. Chen, *Novel single switch dc-dc converter for high step-up conversion ratio*, J. Power Electron., **18**, *3*, pp. 662-671, 2018.
8. O. Ray, S. Mishra, A. Joshi, V. Pradeep, A. Tiwari, *Implementation, and control of a bidirectional high-gain transformer-less standalone inverter*, IEEE Energy Conversion Congress and Exposition (ECCE), 2012, pp. 3233-3240.
9. F.Z. Peng, *Z-source inverter*, Conference Record of the 2002 IEEE Industry Applications Conference, **2**, pp. 775-781, 2002.
10. C.J. Gajanayake, L.F. Lin, G.H. Beng, S.P. Lam, S.L. Kian, *Extended boost Z-source inverters*, 2009 IEEE Energy Conversion Congress and Exposition, pp. 3845-3852.
11. S. Upadhyay, R. Adda, S. Mishra, A. Joshi, *Derivation and characterization of switched-boost inverter*, Proc. of the 2011 14th European Conf. on Power Electronics and Applications, pp. 1-10.
12. S. Mishra, R. Adda, A. Joshi, *Inverse Watkins–Johnson topology-based inverter*, IEEE Trans. Power Electron., **27**, *3*, pp. 1066-1070, 2012.
13. S. Annapoorani, R. Jayaparvathy, *An efficient single stage boost inverter with one cycle control for PV applications*, 2017 IEEE International Workshop on Integrated Power Packaging (IWIPP), pp. 1-5.
14. O. Ray, S. Mishra, *Boost-derived hybrid converter with simultaneous dc and ac outputs*, IEEE Trans. Ind. Appl., **50**, *2*, pp. 1082-1093, 2014.
15. S.S. Nag, R. Adda, O. Ray, S K. Mishra, *Current-fed switched inverter-based hybrid topology for dc nanogrid application*, IECON 2013, 39th Annual Conference of the IEEE Industrial Electronics Society, 2013, pp. 7146-7151.
16. F. Hamza, K. Fateh, T. Billel, L. Abdelbaset, B. Abdesslam, *Sensorless field-oriented control of current source inverter fed induction motor drive*, Rev. Roum. Sci. Techn. – Électrotechn. et Énerg., **63**, *1*, pp. 100-105, 2018.